Immunity
Article

Critical Role for Asparagine Endopeptidase in Endocytic Toll-like Receptor Signaling in Dendritic Cells

Fernando E. Sepulveda,[1,3] Sophia Maschalidi,[1,3] Renaud Colisson,[1] Lea Heslop,[1] Cristina Ghirelli,[1] Emna Sakka,[1] Ana-Maria Lennon-Duménil,[1] Sebastian Amigorena,[1] Lucien Cabanie,[2] and Bénédicte Manoury[1,*]
[1]Institut Curie, U932, 26 rue d'Ulm, 75005 Paris, France
[2]Unité des protéines recombinantes, UMR144, 12 rue Lhomond, 75005 Paris, France
[3]These authors contributed equally to this work
*Correspondence: benedicte.manoury@curie.fr
DOI 10.1016/j.immuni.2009.09.013

SUMMARY

Intracellular Toll-like receptor 3 (TLR3), TLR7, and TLR9 localize in endosomes and recognize single-stranded RNA and nucleotides from viruses and bacteria. This interaction induces their conformational changes resulting in the production of proinflammatory cytokines and upregulation of cell surface molecules. TLR9 requires a proteolytic cleavage for its signaling. Here, we report that myeloid and plasmacytoid dendritic cells (DCs) deficient for the asparagine endopeptidase (AEP), a cysteine lysosomal protease, showed a decrease in the secretion of proinflammatory cytokines in response to TLR9 stimulation in vitro and in vivo. Upon stimulation, full-length TLR9 was cleaved into a 72 kDa fragment and this processing was strongly reduced in DCs lacking AEP. Processed TLR9 coeluted with the adaptor molecule MyD88 and AEP after size exclusion chromatography. When expressed in AEP-deficient DCs, the 72 kDa proteolytic fragment restored TLR9 signaling. Thus, our results identify an endocytic protease playing a critical role in TLR processing and signaling in DCs.

INTRODUCTION

Toll-like receptors (TLRs) recognize microbial products and play an essential role in innate and adaptive immunity. They belong to the type I transmembrane protein family that contains a leucine-rich repeat in an extra cellular loop and a Toll-interleukine-1 (IL-1) receptor (TIR) homology domain in the cytoplasmic tail (Bell et al., 2003). TLRs are divided in two families: TLR1, 2, 4, 5, 6, and 11, which sense the presence of proteins and lipids from bacteria and are expressed at the plasma membrane; and TLR3, 7-8, and 9, localized in endosomes (Kawai and Akira, 2006; Kim et al., 2008), which engage single-stranded and double-stranded RNA and unmethylated CpG DNA, respectively, from pathogens. In the absence of stimulation, TLR9 is retained in the endoplasmic reticulum (ER) together with another ER-resident protein, UNC93B (Brinkmann et al., 2007). Upon stimulation with CpG DNA, it relocates to the endo-lysosomal compartment, allowing the recruitment of the adaptor molecule, MyD88, and thereafter, signals. Recently it was demonstrated that in macrophages, after stimulation, TLR9 is cleaved into a C-terminal fragment and that this cleaved form alone is competent for signaling (Ewald et al., 2008). This is an important step indeed, because it is the activation of the MyD88 signaling pathway that leads to the production of proinflammatory cytokines and cell surface expression of costimulatory molecules in dendritic cells (DCs) (Hemmi and Akira, 2005; Kaisho and Akira, 2001). It has further been shown that interfering with the pH by blocking lysosomal acidification inhibits TLR7 and 9 signaling (Yi et al., 1998), suggesting a role for endocytic proteases in endosomal TLR stimulation.

Lysosomal proteases, which are highly dependent on the pH for their activities, can be classified into three major classes: aspartic, serine, and cysteine protease families. Asparagine endopeptidase (AEP) or mammalian legumain is an asparagine-specific cysteine protease that has been implicated in the MHC class II presentation pathway. AEP initiates the processing of tetanus toxin in human B cells, destroys an immuno-dominant peptide of myelin basic protein (MBP, 85-99), and performs the early steps of degradation of the invariant chain (Ii) in human B-EBV cells (Manoury et al., 1998, 2002, 2003). AEP is unrelated to the papain-like cysteine protease family such as cathepsins B (CatB) and L (CatL); it is grouped together with the caspases, separases, and some bacterial proteases in clan CD (Chen et al., 1997, 1998; Uhlmann et al., 2000). Unlike other lysosomal cysteine proteases, AEP is insensitive to leupeptin and cleaves on the carboxy-terminal sides of asparagine residues. AEP is synthesized as a 56 kDa precursor and targeted to the endocytic pathway. In the lysosomal compartments, N- and C-terminal propeptides are auto-cleaved to generate a 46 kDa mature form, which can be further processed into a 36 kDa fragment (Li et al., 2003). Acidic pH is a prerequisite for maturation of AEP, and therefore its greatest activity is found in lysosomal compartments. AEP is constitutively expressed in most cell types, especially in macrophages and DCs. Recent published findings have centered around cysteine proteases (in particular cathepsin K and cathepsin L) in endosomal TLR activation (Asagiri et al., 2008; Matsumoto et al., 2008; Park et al., 2008). However, no direct biochemical evidence in DCs for TLR9 cleavage by cathepsin L or cathepsin K was brought forward in

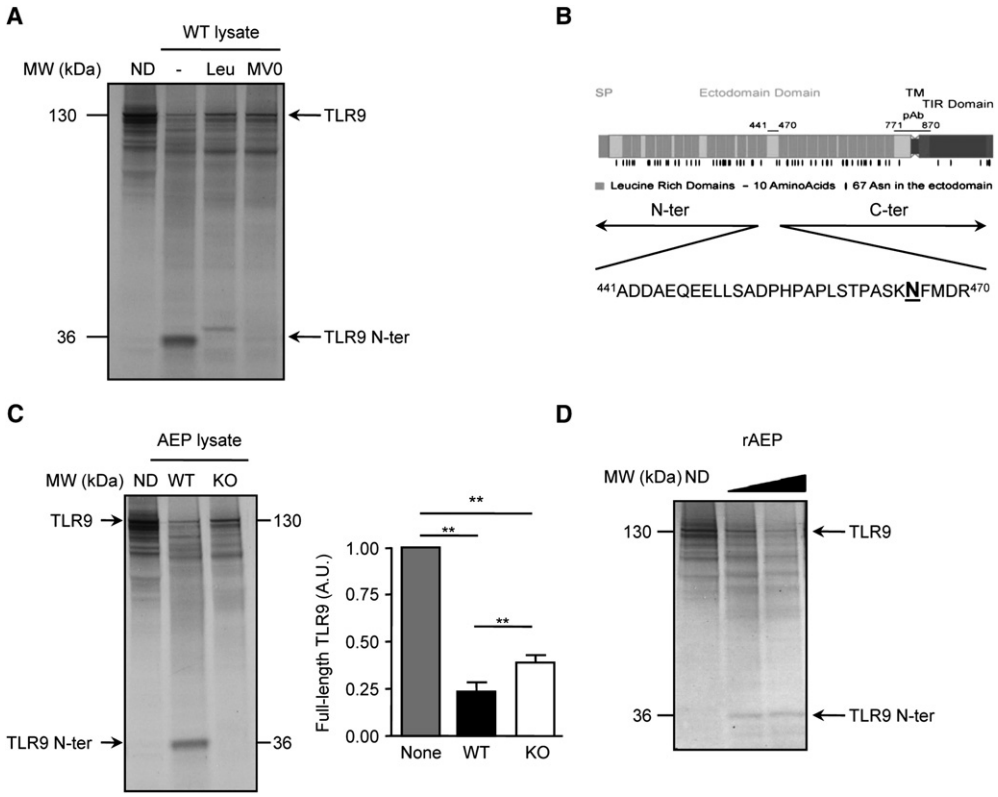

Figure 1. Digestion of ^{35}S-Labeled TLR9 with Purified AEP or Disrupted Lysates from WT or AEP-Deficient BMDCs

(A) *Tlr9* cDNA was transcribed and translated in vitro in the presence of rabbit reticulocyte and ^{35}S-Met. ^{35}S-Met-labeled TLR9 protein was digested or not with 20 μg of WT cell lysate in the absence or presence of the indicated inhibitors for 4 hr.

(B) Scheme of murine TLR9 protein (Uniprot accession number Q9EQU3). The 26 LRRs and recognition domain of polyclonal rabbit TLR9 (Santa Cruz) are represented as well as the putative Asn cleavage site, pI, and MW of fragments.

(C) Same reaction as (A) via WT (lane 2) or AEP-deficient (KO, lane 3) DC lysate (left). Graphs show mean ± SD (n = 3) via one-way ANOVA test. **p < 0.01 (right).

(D) Same digestion experiments with different doses of rAEP (7.5U, lane 2; 15U, lane 3). The reactions were performed in 50 mM citrate buffer, 0.1% CHAPS (pH 5.5) and separated on a 10% SDS-NuPAGE. ND, nondigested.

Representative data from three independent experiments.

those studies. With this in mind, we decided to investigate whether AEP was required for TLR9 response. Here, we showed that full-length TLR9 was a substrate for AEP both in vitro and in living cells. Blocking AEP activity by knocking down its gene decreased the appearance of TLR9 proteolytic fragments of 36 and 72 kDa in murine DCs, resulting in reduced TLR9 signaling after CpG stimulation in cells and in AEP-deficient (*Lgm*$^{-/-}$) mice. Our resulting findings suggest that AEP plays a major role in TLR9 signaling in DCs.

RESULTS

AEP Can Cleave TLR9 In Vitro

To analyze the processing of TLR9 in vitro, we incubated radiolabeled translated TLR9 with lysate of wild-type (WT) bone-marrow-derived DCs (BMDCs) as a source of proteases. The full-length TLR9 protein was digested to produce one major band that migrates around 36 kDa (Figure 1A), corresponding probably to the N-terminal part of TLR9 (TLR9 N-ter) (Figure 1B) previously described (Park et al., 2008). We then used various protease inhibitors to identify the enzymes involved in TLR9 degradation in vitro. In the presence of leupeptin (a broad inhibitor of cysteine proteases except AEP), full-length TLR9 was digested to generate a fragment different from the TLR9 N-ter migrating at a higher molecular weight (Figure 1A). In contrast, addition of MV026630, previously described to specifically inhibit AEP (Loak et al., 2003; Manoury et al., 2003), showed a clear inhibition of the production of the TLR9 N-ter product (Figure 1A). To investigate this further, we used lysate from WT and AEP-deficient BMDCs as a source of proteases. Proteases contained in both lysates were able to degrade full-length TLR9 (Figure 1C), but those expressed in AEP-deficient BMDC lysate digested TLR9 less efficiently than WT lysate. Longer exposure of the radioactive film showed that both lysates could cleave TLR9 into fragments (Figure S1A available online) among which two of them migrate at 72 and 36 kDa corresponding probably to the N- and C-terminal part of TLR9 fragments (Figure 1B). To test whether AEP could directly cleave TLR9, TLR9 was incubated with recombinant AEP, at different doses. Recombinant AEP was able to cleave TLR9 into fragments, one of them being the TLR9 N-ter (Figure 1D). As previously described (Ewald et al., 2008; Park et al., 2008), cathepsins K (CatK), L (CatL), and S (CatS)

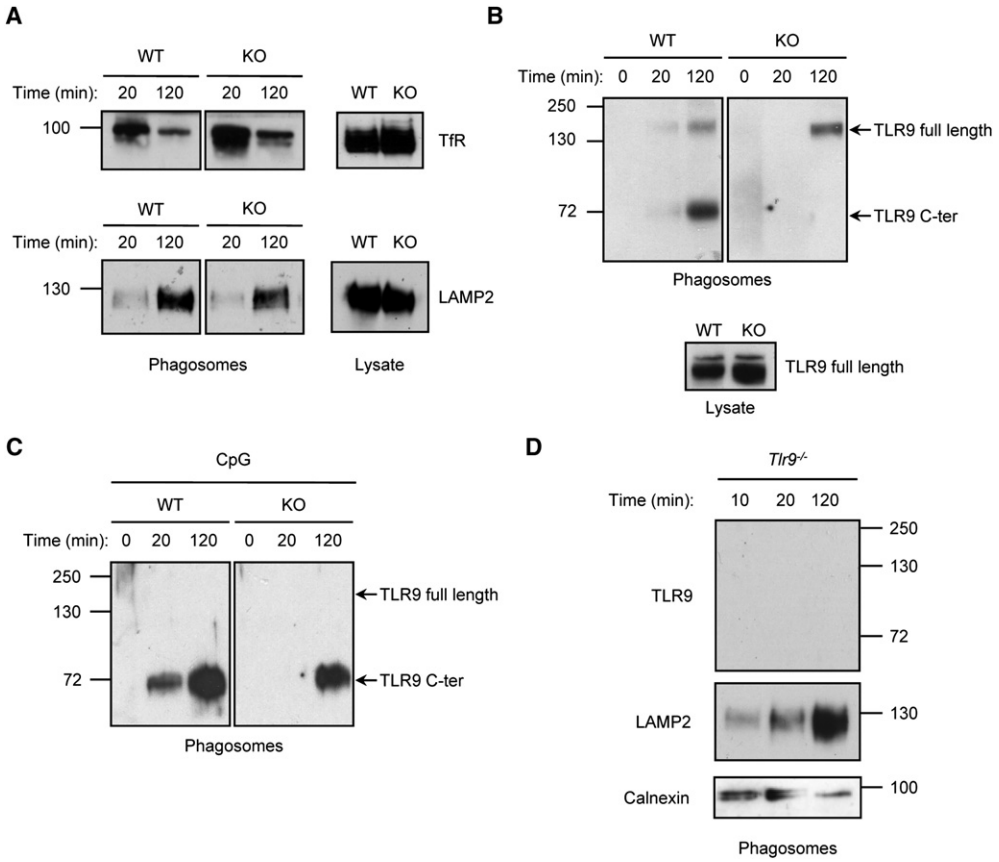

Figure 2. Lack or Severe Delay of TLR9 Processing in Phagosomal Compartments Purified from AEP-Deficient Cells

(A) Phagosomes from WT or AEP-deficient (KO) BMDCs were magnetically purified after 20 min or 2 hr. Proteins expressed either in total lysate (50 μg) or in phagosomes (5 μg) were resolved by SDS-PAGE. Early (TfR) and late (LAMP2) markers were visualized by immunoblot.

(B and C) Immunodetection of TLR9 proteins in early and late phagosomes from WT or AEP-deficient (KO) BMDCs unstimulated (B) or stimulated (C) with CpG.

(D) Same experiments as described in (A) in phagosomes purified from *Tlr9*$^{-/-}$ DCs.

Data are representative of three experiments.

were also able to cleave TLR9 in vitro (Figure S1B) and more efficiently than AEP or CatB. These results show that in vitro, AEP contributes to TLR9 processing and suggest that AEP might play a role in TLR9 processing in living cells.

Compromised TLR9 Cleavage in AEP-Deficient DCs

TLR9 resides in the ER in resting cells and upon stimulation translocates to the endo-lysosomal compartment where it signals. To look at endogenous TLR9 cleavage and intracellular location, we purified phagosomes from WT and AEP-deficient DCs fed with latex beads. As expected, early phagosomes purified after 20 min of pulse with latex beads were enriched in transferin receptor protein (TfR) (Figure 2A, top) and, in contrast, late phagosomes (20 min of pulse followed by 100 min of chase) accumulated LAMP2 protein (Figure 2A, bottom). At the steady state, a TLR9 cleavage fragment of approximately 72 kDa size was observed only in late WT phagosomes (Figure 2B). We designated this fragment as being the C-terminal segment of TLR9 containing at least the last 400 amino acids, based on the recognition site of TLR9 antibody that maps between amino acids 771 and 800 (Figure 1B) and previous experiments showing the accumulation of this TLR9 cleavage fragment in phagosomes purified from raw cells (Ewald et al., 2008). In the presence of CpG, TLR9 cleavage occurred much more rapidly and was already detectable after 20 min of CpG stimulation (Figure 2C). In the absence of AEP, no TLR9 processing fragment was observed at the steady state in either early or late phagosomes (Figure 2B). We did detect the 72 kDa TLR9 cleavage fragment in CpG-stimulated AEP-deficient cells, but at a lower amount and only in late phagosomes (Figure 2C). As expected, no proteins—neither full length nor fragmented—were observed in phagosomes purified from TLR9-deficient (*Tlr9*$^{-/-}$) DCs (Figure 2D). Altogether, these results show that after CpG stimulation, the generation of the TLR9 C-terminal fragment is strongly delayed in phagosomes purified from AEP-deficient cells.

We were not able to detect the adaptor molecule MyD88 either in WT and AEP-deficient phagosomes. Thus, to investigate whether the adaptor MyD88 molecule interacted or coeluted with the processed form of TLR9 in WT and AEP-deficient DCs, we stimulated cells with and without TLR9 ligand for 30 min and then fractionated TLR9 and MyD88, on the basis of size exclusion chromatography. In three separate experiments,

comprising 18 samples, quantitatively similar profiles of total lysate from WT and AEP-deficient cells were obtained (Figure S2). Size exclusion chromatography separated high molecular weight components into two major peaks where UV absorbance was detected. Peak 1 (fractions 12 to 18), corresponds to proteins that eluted at a high molecular weight ranging from 800 to 2000 kDa. Full-length TLR9 (~130 kDa), as well as other polypeptides that most likely correspond to dimers or complexes of TLR9 (~200 kDa) that resist to nonreducing conditions used here (Figure 3A), were detected in these fractions in WT and AEP-deficient BMDCs at the steady state. We next investigated the fate of TLR9 after CpG treatment. After 30 min of CpG stimulation, full-length TLR9 was still observed in fractions 12 to 18 (Figure 3B) from WT DCs, but also, a TLR9 cleavage fragment of approximately 72 kDa size was detected in fractions 36 to 41 corresponding to proteins of molecular weight of approximately 70 to 200 kDa. In the absence of AEP, after CpG stimulation, we did not detect this 72 kDa TLR9-processed fragment (Figure 3B). In these cells, we consistently observed an accumulation of uncleaved full-length TLR9 (Figure 3B). Same results were obtained after 60 min of CpG stimulation (data not shown). We then investigated whether or not the adaptor MyD88 molecule coeluted with the processed form of TLR9 (fractions 36 to 41) in WT DCs. Indeed, we were able to detect MyD88 in these fractions (36–41, Figure 3B). In contrast, we were unable to detect any coelution between MyD88 and full-length TLR9 either in WT or AEP-deficient DCs both at steady state and after CpG stimulation (Figures 3A and 3B, fractions 12 to 18). After 30 min of CpG stimulation, we observed a substantial enrichment in the amount of 72 kDa TLR9 fragment (in fraction 40) in WT compared to AEP-deficient BMDCs (Figure 3C). No TLR9 protein, neither full length nor fragmented, was detected in fractionated *Tlr9*$^{-/-}$ cells at the steady state or stimulated with CpG (Figure S3). Additionally, in LPS-activated cells, no cleavage of TLR9 was observed in the fractions 41–49 where MyD88 was detected (Figure S4). Taken together, these results demonstrate that CpG stimulation induces a TLR9 cleavage product of 72 kDa that coelutes with MyD88 in WT cells, and that at early time points of CpG stimulation, AEP-deficient DCs fail to process TLR9, suggesting an impaired association between cleaved TLR9 and the adaptor molecule MyD88 in these cells.

CpG Boosts the Recruitment and Activity of AEP and Decreases the Endosomal pH

The above results suggested that TLR9 processing might occur more rapidly after CpG stimulation. We hypothesized that CpG induced the recruitment and/or a boost in protease activities that promote TLR9 cleavage. To address this question, we measured the recruitment and/or activity of AEP both in cells and in endo-lysosomal compartments after CpG stimulation. At steady state, AEP was coeluted with MyD88 (Figure 3A, fractions 36–41) and not with full-length TLR9 (Figure 3A, fractions 12–18). After TLR9 stimulation, enhanced mature AEP was detected in the same fractions where TLR9 cleavage fragment accumulated (Figure 3B, fractions 36–41). No AEP was detected in AEP-deficient DCs (Figures 3A and 3B). Upon CpG stimulation, there was a substantial accumulation of AEP in the same fraction where the C-terminal TLR9-processed fragment appears (Figure 3C). Furthermore, coelution of AEP with processed TLR9 and MyD88 correlated with a strong increase in AEP activity observed in both total cell extracts and endosomes, where cleavage of TLR9 occurred after CpG stimulation (Figure 3D). Thus, CpG stimulation increases AEP activity and recruitment in compartments where TLR9 is cleaved.

Because AEP is active at low pH, we analyzed whether this boost in AEP activity correlates with an increased acidification in endosomes and lysosomes. We observed a dramatic acidification of the endocytic pathway upon TLR9 activation in WT and AEP-deficient DCs (Figure 3E). As expected, drugs interfering with pH acidification, such as concanamycin B (data not shown), completely blocked TLR9 signaling (Figure 3F). Thus, TLR9 processing requires low pH and AEP activity.

AEP Is Required for Full Cytokine Production in DCs

The above results suggested that the lack of AEP activity might decrease TLR9 signaling. To address this question, WT and AEP-deficient BMDCs were stimulated with TLR4 and TLR9 agonists. We observed a significant decrease in tumor necrosis α (TNF-α) and interleukin 6 (IL-6) secretion by AEP-deficient DCs upon TLR9 engagement, but not when TLR4 was stimulated (Figures 4A and 4B). Similar results were obtained when we used DCs preincubated with MV026630 (data not shown). In contrast, we did not observe any difference in TNF-α secretion when WT or AEP-deficient macrophages were stimulated with TLR4 or TLR9 agonists (Figure S5). We next investigated whether the TLR9 C-terminal fragment, which contains the cytoplasmic TIR domain that interacts with MyD88, was able to initiate TLR9 signaling. As previously described (Park et al., 2008), the C-terminal fragment of TLR9 was sufficient to initiate signaling to the same level as full-length TLR9 when expressed in *Tlr9*$^{-/-}$ DCs (Figure 4C). Neither C-terminal nor full-length TLR9 could restore signaling in cells lacking MyD88 (Figure 4D). Importantly, AEP-deficient DCs transfected with cDNA encoding the recombinant C-terminal TLR9 product regained responsiveness to the same level as WT cells after CpG stimulation, as indicated by IL-6 secretion (Figure 4E, left). As shown above, after TLR9 stimulation, diminished IL-6 production was detected when AEP-deficient DCs were transfected with cDNA encoding GFP control plasmid or GFP-tagged full-length TLR9 (Figure 4E, left) as compared to WT cells. Furthermore, transfection of cDNAs coding for AEP and GFP in AEP-deficient DCs restore IL-6 secretion after TLR9 stimulation (Figure 4E, left). Same results were obtained when IL-12p40 expression was measured (Figure 4E, bottom). As a control, LPS-stimulated cells either transfected with GFP, full-length, or C-terminal TLR9 plasmids secreted same amount of IL-6 and IL-12p40 (Figure 4E, right panels). We conclude that AEP plays a critical role in TLR9 signaling in DCs and that the C-terminal TLR9 fragment alone is sufficient to restore signaling in AEP-deficient DCs to the same level as in WT cells, requiring the adaptor molecule MyD88.

Altered CpG Adjuvancy in AEP-Deficient Mice

To examine the role that AEP might play in vivo in TLR9 signaling in DCs, we assessed the ability of AEP-deficient DCs to secrete proinflammatory cytokines and to prime naive CD4$^+$ T cells. It has been shown that cytokines are mainly secreted in vivo by CD11c$^+$ DCs in the early hours after TLR agonist injection in

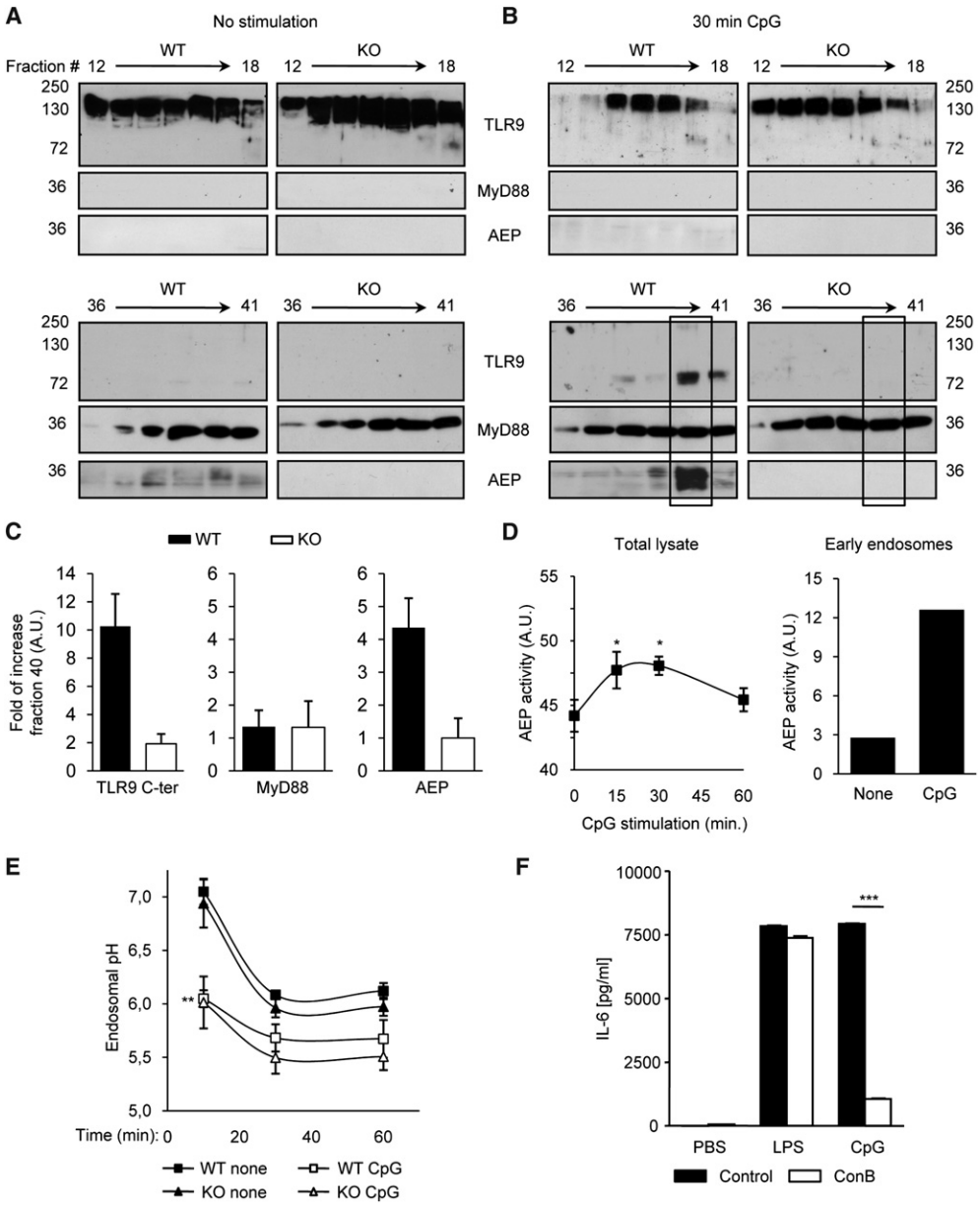

Figure 3. CpG Induces TLR9 Processing in an AEP-Dependent Fashion and a Rapid Decrease of Endosomal pH in WT and AEP-Deficient Dendritic Cells

(A and B) Lysates from WT (left) or AEP-deficient (KO) BMDCs (right) treated (B) or not (A) with CpG (10 μg/ml) for 30 min, were applied to a size exclusion resin and eluted with 150 mM NaCl, 50 mM Tris (pH 7.4), 5 mM $MgCl_2$. Fractions were collected and were analyzed (5 μg) on a 10% Bis-Tris NuPAGE gel. TLR9, MyD88, and AEP proteins were visualized by immunoblot with TLR9-, MyD88-, and AEP-specific antibodies.

(C) Quantification of the fold of increase of the TLR9 processing fragment (C-ter), MyD88, and AEP proteins present in fraction 40 upon CpG stimulation via Image J Software. Graphs show mean ± SD (n = 3).

(D) AEP activity in total lysate and purified endosomes from WT BMDCs treated or not with CpG (10 μg/ml) for the indicated time was measured with a specific fluorescent substrate. Graphs show mean ± SD (n = 3) via unpaired t test. *$p < 0.05$.

(E) Kinetic of endo-lysosomal pH in WT and AEP-deficient (KO) BMDCs pulsed for 10 min with FITC- and Alexa-647 coupled dextran in the presence or not of 10 μg/ml of CpG and chased for different times. Graphs show mean ± SD (n = 3) via unpaired t test. **$p < 0.01$.

(F) Effect of endosomal alkalinisation in cytokine secretion upon LPS or CpG stimulation in WT BMDCs. Graphs show mean ± SD (n = 3) via unpaired t test. ***$p < 0.001$.

mice (Hou et al., 2008). Cytokine production from DCs in vivo was then examined 2 hr after the mice were i.v. injected with CpG or LPS. In WT mice, both LPS and CpG induced IL-6 and IL-12p40 secretion (Figures 5A and 5B). In contrast, we consistently observed attenuated IL-6 and IL-12p40 secretion in AEP-deficient mice after TLR9 stimulation (Figures 5A and 5B).

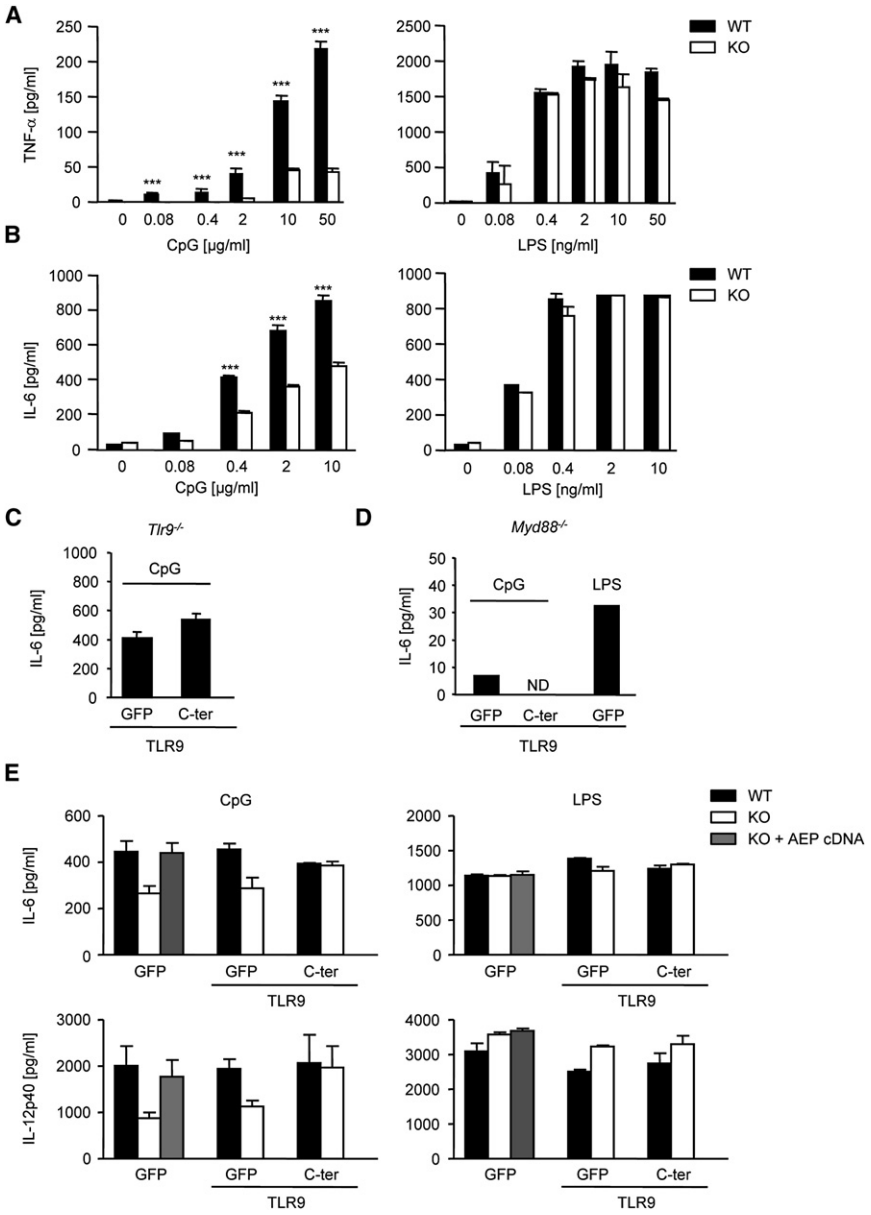

Figure 4. AEP Activity Is Required for Full Cytokine Production after TLR9 Stimulation

(A and B) BMDCs from WT (black bars) or AEP-deficient (KO) (white bars) mice were stimulated with increasing concentrations of TLR agonist (CpG for TLR9, LPS for TLR4) for 6 hr, and secretion of TNF-α and IL-6 were measured by ELISA. Graphs show mean ± SD (n = 3) via unpaired t test. ***$p < 0.001$.

(C–E) *Tlr9*$^{-/-}$ (C) *Myd88*$^{-/-}$ (D) AEP-deficient (KO, white bars) and WT (black bars) (E) DCs were transfected with cDNAs encoding GFP, GFP-tagged full-length TLR9, or C-terminal TLR9 fragment and/or AEP (gray bars) at day 8 of culture. After transfection, cells were harvested and stimulated with TLR ligands (CpG, 2 μg/ml; LPS, 10 ng/ml) for 16 hr and secretion of IL-6 (top) and IL-12p40 (bottom) was measured by ELISA. Amount of IL-6 and IL-12p40 produced by unstimulated cells was subtracted from CpG-stimulated cells. (ND, not detected). Graphs show mean ± SD (n = 3).

Thus, in DCs, AEP is required for the secretion of inflammatory cytokines induced by TLR9 engagement by CpG in vivo.

To monitor how decreased TLR9 signaling in AEP-deficient DCs could affect their capacity to initiate adaptive immune response, we measured the activation of ovalbumin (OVA)-specific TCR transgenic OTII T cells after injection in WT and AEP-deficient mice. First, we excluded that OVA processing was dependent on AEP both in vitro and in vivo. Ovalbumin degradation assays were performed as previously described (Savina et al., 2006). As shown in Figure S6A, antigen degradation was observed over time and was equivalent in WT and AEP-deficient BMDCs. To investigate antigen presentation of OVA in vivo, we immunized WT or AEP-deficient mice with OVA. Ten days later, lymph nodes were restimulated in vitro with different OVA concentration and T cell proliferation was measured by ^{3}H-thymidine incorporation. OVA-specific T cell responses generated in WT or AEP-deficient mice were again similar (Figure S6B). These results indicate that OVA processing in vitro and in vivo does not require AEP.

To evaluate the capacity of AEP-deficient DCs to activate T cells in response to TLR9 agonist in vivo, we injected CFSE-labeled OT-II T cells into WT and AEP-deficient mice and then immunized them with OVA-coated beads alone or with soluble CpG or LPS used as adjuvants. T cell proliferation was analyzed 2 days later. In WT mice, both immunization protocols (CpG and LPS) led to a proliferation and an accumulation of OT-II T cells in the spleen compared to immunization with OVA alone (Figures 5C and 5D). In AEP-deficient mice, we observed a normal proliferation and accumulation of OT II T cells in response to LPS treatment compared to WT mice (Figures 5C and 5D). However, fewer OT-II T cells accumulated in the spleen of AEP-deficient mice that were immunized with CpG than in the control mice (Figure 5D). In fact, no proliferation of OT-II T cells was seen when CpG was used as an adjuvant in AEP-deficient mice (Figure 5C, left bottom). Thus, AEP-deficient mice show an altered response to TLR9 in vivo, characterized by a defect in inflammatory cytokine secretion and impaired capacity to initiate an adaptive immune response upon TLR9 activation.

Reduced Cytokine Production in Plasmacytoid DCs Lacking AEP

We then wondered whether this defect in TLR9 signaling in cells lacking AEP was a specific feature of myeloid DCs. We purified mouse and human plasmacytoid DCs, key cells in the immune system that secrete interferon α (IFN-α) after viral infection.

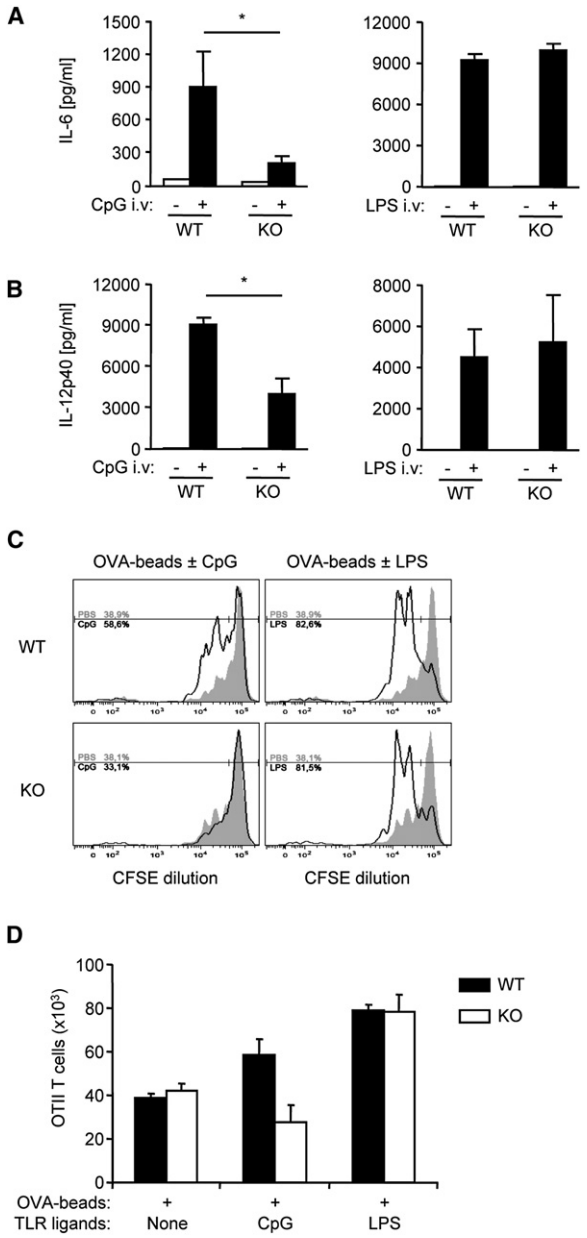

Figure 5. Impaired CpG Adjuvancy in AEP Knockout Mice

(A and B) IL-6 (A) and IL-12p40 (B) secretion were measured in serum of WT or AEP-deficient (KO) mice after 2 hr of injection i.v. with CpG-B (25 μg) (left), LPS (1 μg) (right), or vehicle alone (PBS). Graphs show mean ± SD (n = 3 via unpaired t test). *$p < 0.05$.

(C and D) In vivo proliferation assay of congenic CFSE-labeled OTII T cells (Thy1.1$^+$). Lymphocytes were transferred into Thy1.2$^+$ WT (black bars) or AEP-deficient (KO) mice (white bars) 8 hr before injection of OVA-coated beads i.v. with or without soluble TLR agonist. CFSE dilution and total number of OTII cells in the spleen were measured by flow cytometry. Graphs show mean ± SD (n = 3). Data are representative of three experiments.

Upon CpG stimulation, human and mouse pDCs preincubated with MV026630 showed a substantial decrease in IFN-α production compared to nontreated cells (Figures 6A and 6B). As previously shown, the inhibitor of PI3-kinase (LY compound) blocked IFN-α secretion upon CpG stimulation (Guiducci et al., 2008) and to the same extent as the AEP inhibitor (Figure 6B). Thus, AEP plays a critical role in TLR9 signaling not only in myeloid DCs but also in plasmacytoid DCs.

Cathepsin Activity Is Not Impaired in DCs Lacking AEP

To examine whether expression and activity of other cysteine proteases might be altered by the loss of AEP as reported (Maehr et al., 2005; Shirahama-Noda et al., 2003) and thus influence TLR9 processing, we performed CatB, CatK, CatL, and CatS immunoblots on samples from WT and AEP-deficient BMDCs. Whereas the immature and mature form of CatB and the two-chain form (heavy and light chain) of CatL were present in WT, only the immature CatB and single-chain CatL form could be detected in AEP-deficient cells (Figure 7A). No difference in CatS expression was observed. Interestingly, CatK expression was greatly increased in AEP-deficient cells in comparison to WT, where it was almost undetectable (Figure 7A). Active forms of cathepsins in BMDCs can be identified by taking advantage of their reaction to the cysteine-protease mechanism-based probe, DCG-04 (Lennon-Dumenil et al., 2002; Maehr et al. 2005). BMDC lysates from WT and AEP-deficient cells were labeled with DCG-04 and immunoprecipitated for CatB, L, and S (Figure 7B) proteins. These data revealed that CatB, L, and S in AEP-deficient cells were as enzymatically active as those in WT cells based on their labeling with the probe DCG-04. Additionally, by using fluorogenic substrates selective for CatB, CatB or CatL, and CatS, we found a similar (CatB and CatS) or, in some cases, an increased (CatB or CatL) amount of hydrolysis of these substrates in AEP-deficient cells (Figure 7C). After CpG stimulation, WT or AEP-deficient DCs showed an overall enhancement in cysteine protease activity (Figure 7C). To rule out a role for CatK in TLR9 processing in AEP-deficient cells, we fed them with pro-CatK to see whether it could restore TLR9 signaling upon CpG stimulation. Despite enhanced amount of CatK in AEP-deficient cells (Figure 7D), this protease was not able to restore IL-12p40 secretion after CpG stimulation (Figure 7E). Altogether, these results suggest that changes in the activity of cysteine proteases such as CatB, K, L, and S are not responsible for decreased TLR9 response in AEP null cells.

Mutating Putative AEP Cleavage Site in TLR9 Decreases TLR9 Response in Living Cells

The strict specificity of AEP can allow us to identify and mutate protease cleavage sites in TLR9 protein. Although a 3D structure for TLR9 is not known, secondary-structure prediction programs are available for the residues 441–470 situated between the two leucine-rich regions (LLR 14–15) described previously as being part of a flexible loop susceptible to proteolysis (Park et al., 2008). Indeed, TLR9 contains one asparagine localized in this region that can be a putative cleavage site for AEP (Figure 1B). To establish whether or not AEP could cleave TLR9 at this putative site, site-directed mutagenesis was performed on asparagine residue 466 that was mutated to Gln (N466Q). N466Q TLR9 was subjected to AEP digestion in vitro and was slightly more resistant to AEP degradation than WT TLR9 (data not shown). We next investigated whether or not this TLR9 mutant was able to initiate TLR9 signaling. WT or N466Q TLR9 cDNAs were transfected into *Tlr9*$^{-/-}$ cells and cytokine production

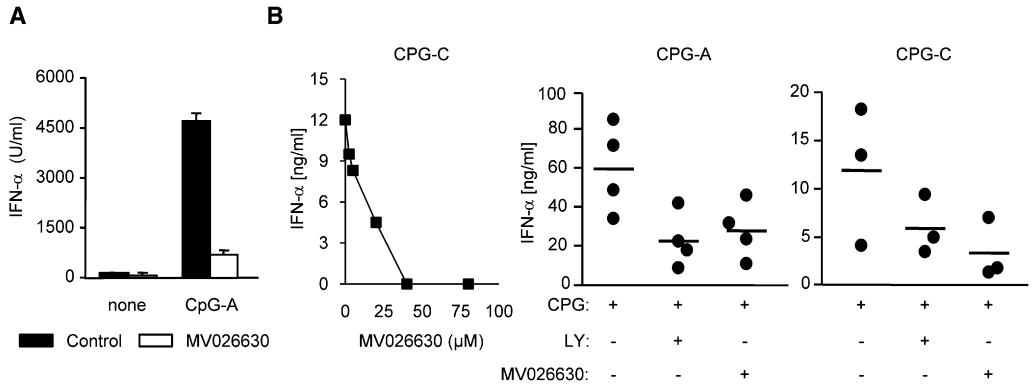

Figure 6. Impaired Cytokine Secretion upon AEP Inhibition in Plasmacytoid Dendritic Cells

(A) Spleen-derived plasmacytoid DCs were treated with or without MV026630 (20 μM) and activated with 10 μg/ml of CpG-A. IFN-α secretion was measured by ELISA after overnight culture. Graphs show mean ± SEM (n = 3).

(B) Human pDCs isolated from fresh buffy coats were stimulated overnight with CpG-A or CpG-C (5 μg/ml) in the presence or absence of MV026630 (20 μM or at different concentrations) or PI3K (LY, 5 μM). IFN-α secretion was measured by ELISA. Each dot corresponds to pDCs purified from one buffy coat.

was measured upon CpG stimulation. Transfection efficiency was the same for both constructs (~20%) (data not shown). We observed a clear decrease in IL-6 and IL-12p40 production after TLR9 stimulation when TLR9 mutant was expressed in *Tlr9*$^{-/-}$ cells (Figure 7F). As a control, LPS-stimulated cells either transfected with N466Q or WT TLR9 secreted similar amount of IL-6 and IL-12p40 (Figure 7F). These results demonstrate that mutating a putative AEP cleavage site in TLR9 strongly decreases its signaling in DCs, suggesting perhaps direct cleavage of TLR9 by AEP.

DISCUSSION

Drugs interfering with the endo-lysosomal compartments and/or pH acidification, such as chloroquine and concanamycin B, completely block intracellular TLR signaling (Ahmad-Nejad et al., 2002), indicating a possible role of proteases in this process. Although very recent work has shed light on the cleavage of TLR9 in raw transfected cells, few biochemical and in vivo studies exist on the nature of the protease(s) when executing this proteolysis in DCs. We demonstrate here that TLR9 endogenous processing in DCs is dependent on AEP. By using cell fractionation based on protein size, we show that TLR9 is cleaved into a C-terminal fragment that coelutes with the adaptor protein MyD88. Specific inhibition of AEP compromised TLR9 processing and shows that upon CpG stimulation in DCs and in mice, AEP is involved in TLR9 signaling. Consistent with this finding, we observe that TLR9 C-terminal product, once generated, is sufficient to restore TLR9 signaling in AEP-deficient DCs to a similar level as in WT cells.

AEP has a central role in regulating other proteases. Indeed, AEP-deficient cells exhibit a defect in maturation of many cathepsins (CatB, D, H, and L) in kidney and bone marrow, as well as in spleen DCs and BMDCs (Maehr et al., 2005; Shirahama-Noda et al., 2003). These lysosomal proteases reach endocytic compartments as proforms or zymogens where their propeptide is removed proteolytically. The resulting immature or single-chain forms are then cleaved into mature or two-chain forms for CatB and L, respectively. AEP is involved in this latter event of cathepsin maturation through a still unknown process. Thus, the defect in TLR9 processing in AEP-deficient cells could result from the impaired maturation of these cysteine proteases. However, we argue against this hypothesis because: (1) activities and localization of CatB and L in AEP-null cells are unchanged or even increased compared to WT cells, (2) leupeptin, a broad inhibitor of cysteine proteases except AEP, had relatively little effect on TLR9 degradation in vitro, and (3) incubation of AEP-deficient DCs with pro-CatK did not restore TLR9 signaling upon CpG stimulation despite high amount of this enzyme in AEP-deficient cells. However, differential substrate specificity between immature and mature cathepsins could account for the suppressed TLR9 processing observed in AEP-deficient cells. Interestingly, we have noticed that in Ii-deficient cells which display no mature CatL, TLR9 signaling is unaffected (data not shown) (Fiebiger et al., 2002; Lennon-Dumenil et al., 2001). So, altogether these data are not in favor of a participation of cathepsins to the impaired TLR9 signaling observed in DCs lacking AEP.

The strict specificity of AEP has allowed us to identify and mutate a putative AEP cleavage site in the flexible loop of TLR9 protein previously described to be susceptible to proteolysis (Park et al., 2008). Experiments addressing the functionality of this TLR9 mutant in TLR9-deficient cells clearly show a decrease in TLR9 signaling when this mutant was stimulated with CpG, suggesting a direct cleavage of TLR9 by AEP. However, we stress that the exact AEP cleavage site(s) in TLR9 remain to be identified. Because AEP cleaves native antigens, it is tempting to speculate that TLR9 processing requires a first cleavage at an Asn site in endosomes, further allowing other proteases to process and generate a fully active TLR9 fragment in lysosomes. This may explain why cells chemically inhibited with specific cathepsin inhibitors or deficient for these proteases (CatB, K, L, and S) display altered TLR9 signaling in vitro as in AEP-deficient DCs (Asagiri et al., 2008; Ewald et al., 2008; Park et al., 2008). Consistent with this hypothesis, we found an inhibition of IL-6 production in CatB- and L-deficient DCs but to a lesser extent than in AEP-deficient cells (data not shown). In addition, after 15 min of stimulation, CpG induces a strong boost in AEP activity

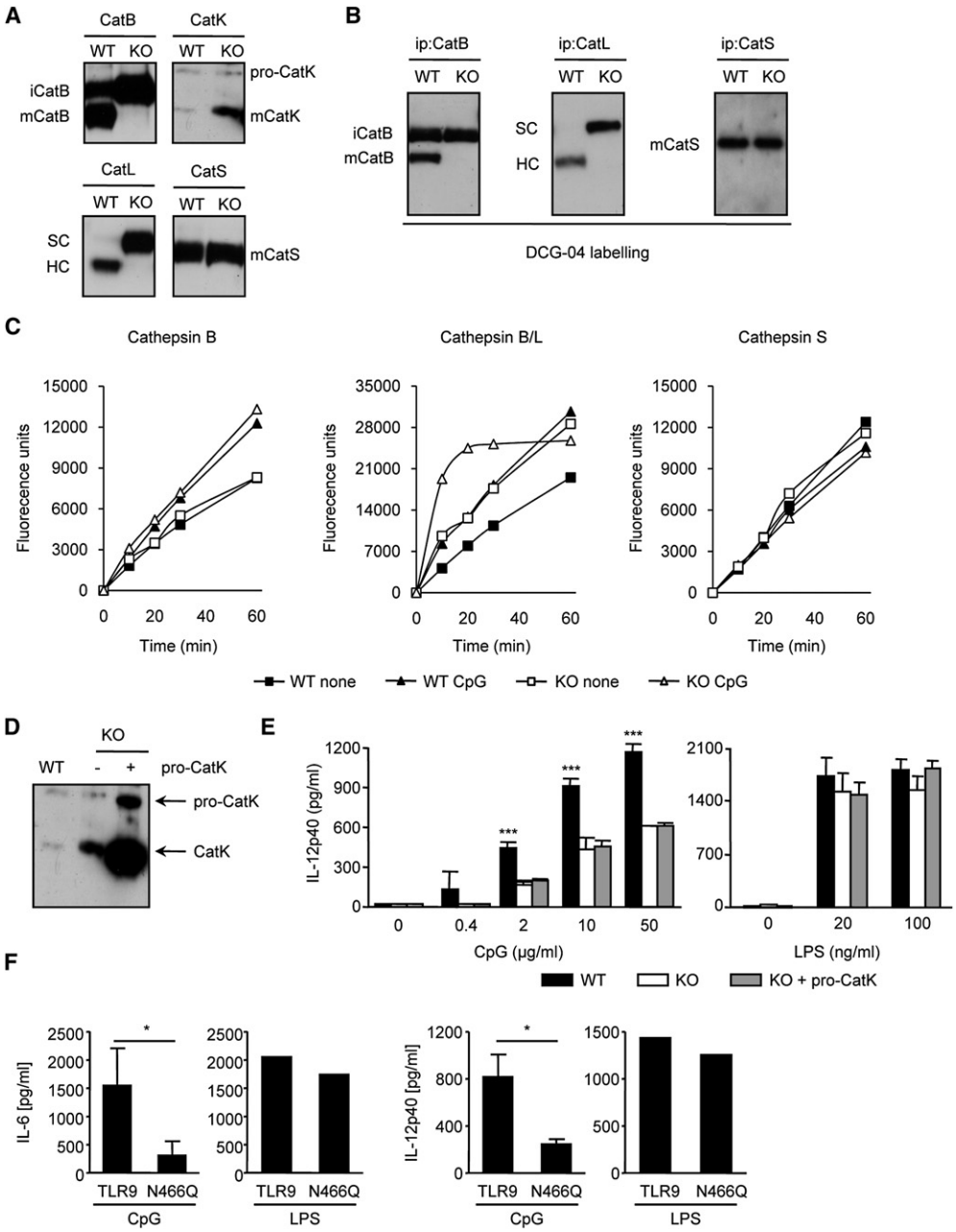

Figure 7. TLR9 Response Is Not Dependent on Cathepsins in AEP-Null Cells whereas Mutating a Putative AEP Cleavage Site in TLR9 Decreases Its Signaling

(A) Protein lysates (20 μg) from WT or AEP-deficient (KO) cells were immunoblotted with antibodies for CatB (top left: iCatB, immature CatB; mCatB, mature CatB), CatK (top right: pro-CatK; mCatK, mature CatK), CatL (bottom left: SC, single chain of CatL; HC, heavy chain of CatL), and CatS (bottom right).

(B) Cysteine proteases activities from WT or AEP-deficient (KO) BMDCs were monitored with the active site labeling probe DCG-04 that react with their catalytic site. CatB, L, and S were analyzed by immunoprecipitation from DCG-04-labeled BMDC lysates and detection of the biotinylated probe with a streptavidin-linked HRP.

(C) Protein lysates (10 μg) of unstimulated (square) or CpG-stimulated (triangles) DCs from WT (black symbols) and AEP-deficient (KO) (white symbols) were assayed for protease activities with specific substrates for CatB, CatB or CatL, and CatS.

(D) Immunoblot analysis for CatK expression of protein lysates from CpG-activated WT or AEP-deficient (KO) BMDCs fed or not with pro-CatK.

(E) Cells were treated as in (D) and stimulated with different concentrations of CpG for 4 hr, and IL-12p40 secretion was measured by ELISA. Graphs show mean ± SD (n = 3) via unpaired t test. ***$p < 0.001$.

(F) *Tlr9*$^{-/-}$ DCs were transfected with cDNAs encoding GFP-tagged full-length or N466Q TLR9 at day 8 of culture. 24 hr after transfection, cells were harvested and stimulated with TLR ligands (CpG, 2 μg/ml; LPS, 10 ng/ml) for 16 hr, and secretion of IL-6 (left) and IL-12p40 (right) was measured by ELISA. Amount of IL-6 and IL-12p40 produced by unstimulated cells was subtracted from CpG-stimulated cells. *$p < 0.05$.

Data are representative of two to three experiments.

that is less pronounced for CatB and L. Interestingly, the increase in cathepsins B and L activity or recruitment in lysosomes occurred at later time points after 60 min of TLR9 stimulation.

The need for proteases in intracellular TLR activation may be a common phenomenon. Indeed, we have evidence that TLR7 is cleaved in DCs upon imiquimod stimulation and that this TLR7 processing might also require AEP. In other words, AEP may be necessary for TLR7 signaling (data not shown).

We did not observe any difference in cytokine secretion when WT or AEP-deficient macrophages were stimulated with TLR9 ligand. The reasons why TLR9 signaling does not rely on AEP in macrophages is not clear. It is most likely that the highly proteolytic, very acidic milieu found in the endocytic pathway of macrophages and which is not observed in DCs negates the dependence of signaling on single proteases. Indeed, we know that the cleavage reported herein is also required for signaling in macrophages (Ewald et al., 2008) and that the neutralization of their endocytic pathway with weak bases also inhibits TLR9 signaling in these cells. In contrast, DCs bear low amounts of lysosomal proteases (Delamarre et al., 2005; Lennon-Dumenil et al., 2002) and inefficient endosomal and lysosomal acidification (Jancic et al., 2007; Trombetta et al., 2003). Because AEP is active at low pH, it is likely that the boost in AEP activity observed upon TLR9 activation but not with TLR4 stimulation (data not shown) results from the enhanced endo-lysosomal acidification. In line with this, at physiological pH, TLR9 binding to CpG DNA is weak, but lowering the pH to 6.5 or 5.5 leads to a strong TLR9-CpG DNA interaction (Rutz et al., 2004). As expected, drugs interfering with pH acidification, such as concanamycin B, completely blocked TLR9 signaling. This can be explained either by a reduced TLR9 processing because AEP is not active enough or/and by a direct inhibition of CpG binding to TLR9. This would point to the conclusion that TLR9 processing requires both low pH and high AEP activity. The fast pH acidification upon CpG stimulation we noticed might allow AEP- and cathepsin-dependent TLR9 cleavage to proceed, quickly followed by a better binding of CpG to TLR9 and a change in receptor conformation. Altogether these events are presumably sufficient to recruit the adaptor molecule MyD88 and initiate signaling.

TLR9 self-associates in cells and is preformed as a dimer (Latz et al., 2007). Upon stimulation with CpG, TLR9 in association with UNC93B relocates to the endo-lysosomal compartment, allowing the recruitment of the adaptor molecule MyD88, and thereafter, signaling. However, it has been suggested (Brinkmann et al., 2007; Kim et al., 2008) that TLR9 can also traffic to endosomes upon LPS stimulation. We have not studied TLR9 trafficking in LPS-stimulated cells, but taking in consideration that pH and protease activities are the same as in WT cells, it seems unlikely that TLR9 processing occurs in LPS-treated cells.

In DCs, upon receptor activation, TLR9 might be associated within a large receptor complex containing MyD88, AEP, other signaling molecules, and chaperones like UNC93B stabilizing these interactions (as we saw in the size exclusion chromatography experiment). Coimmunoprecipitation experiments need to be addressed to confirm the interaction between cleaved TLR9, AEP, and UNC93B. However, early events initiated by CpG DNA recognition in DCs leading to the trafficking of TLR9-UNC93B to the endosomes remain unresolved.

Altogether, our results highlight the primordial role of endocytic proteases, in particular AEP, not only in processing of exogenous antigens for MHC class II presentation pathway, but also in TLR signaling, by perhaps direct proteolysis of endosomal TLRs. Potent and specific AEP inhibitors have already been developed, and might be used as therapeutic tools in viral and inflammatory diseases.

EXPERIMENTAL PROCEDURES

Mice and Cell Preparation

AEP-deficient mice were generated in the lab of C. Peters (Freiburg, Germany) and backcrossed 11 times on B6 background. Transgenic mice that express an OVA-specific TCR (OTII) have been previously described (Barnden et al., 1998). Animals were bred in a pathogen-free environment and were used according to the guidelines and regulations of the French Veterinary Department.

Preparation of BMDCs, Macrophages, and Plasmacytoid DCs

Bone-marrow-derived DCs were generated from WT and AEP-deficient mice by culturing precursors for 7–14 days in GM-CSF-supplemented medium as previously described (Savina et al., 2006). Bone-marrow-derived macrophages were cultured for 6 days in M-CSF-supplemented medium as previously described (Savina et al., 2006). Cell differentiation was controlled by FACS staining for CD11c (HL3), CD11b (M1/70), and F4/80 (6F12) antibodies (all from BD Biosciences). Buffy coats were obtained from adult healthy donors at the Saint-Antoine Crozatier Blood Bank. Human pDCs were isolated by using positive selection BDCA-4-conjugated beads (Miltenyi Biotec), as previously described (Duramad et al., 2005). Mouse splenic pDCs were isolated with mPDCA-1-based positive selection kit (Miltenyi Biotech). Human pDCs were 94%–99% $BDCA2^+$ $CD123^+$, and murine pDCs were more than 90% $mPDCA\text{-}1^+$ determined by flow cytometry.

For cytokine secretion assays, cells were plated in 96-well plate and treated with the indicated concentration of the respective compound for 6 hr. Cytokine concentration was measured in culture supernatants with home-made (IFN-α and TNF-α) or commercial (IL-6 and IL-12p40, eBioscience) ELISA kits. LPS was from Sigma-Aldrich, CpG-B (5′-TGACTGTGAACGTTCGAGATGA-3′) was from Trilink Biotechnologies, and CpG-A (5′-GGTGCATCGATGCAGGGGGG-3′) and CpG-C (5′-TCGTCGAACGTTCGAGATGAT) were a gift from V. Soumelis (Institut Curie, Paris, France). AEP inhibitor (MV026630) was kindly provided by H. Overkleeft (Leiden, Netherlands).

In Vivo DC Stimulation and T Cell Proliferation Assay

Mice were injected i.v. with TLR agonist or PBS alone and bled 2 hr later. Serum cytokine concentration was assessed by ELISA. Mice received 3×10^6 CFSE-labeled lymphocytes i.v. isolated from lymph nodes of Thy1.1 OT II transgenic $Rag^{-/-}$ mice 8–12 hr before injection of OVA-coated beads with or without TLR agonists as adjuvant. CFSE dilution of injected T lymphocytes in spleen was analyzed by staining with anti-CD4 (L3T4) and anti-Thy1.1 (OX-7) (BD PharMingen) 48 hr later. Stained cells were acquired on a FACSCalibur and analyzed with CellQuest (BD Biosciences) or FlowJo (Treestar) software.

Size Chromatography Exclusion, Phagosome Purification, Protease Activity Measurement, and Immunodetection

50×10^6 BMDCs were harvested and stimulated in the presence or absence of CpG (10 μg/ml) or LPS (1 μg/ml) for different time. Cells were then lysed in 50 mM Tris (pH 7.4), 150 mM NaCl, 5 mM $MgCl_2$, 0.5% NP40 for 30 min on ice and centrifuged at 90,000 rpm. The extract was then applied to a G-200 Sephadex size exclusion column (Pharmacia) and equilibrated in 50 mM Tris (pH 7.4), 150 mM NaCl, 5 mM $MgCl_2$. Fractions were eluted with the same buffer and 5 μg of protein was tested for TLR9, MyD88, and AEP expression by western blot.

For phagosome preparation, 50×10^6 BMDCs were pulsed for 20 min at 37°C with magnetic particles (Invitrogen) and then chased at 37°C for 100 min in the presence or absence of CpG (10 μg/ml). For endosome purification, cells were pulsed for 30 min at 4°C with magnetic nanoparticles (kindly given by C. Menager, Jussieu, Paris, France) and chased at 37°C for 30 min with CpG (10 μg/ml). Cells were then washed with PBS and mechanically disrupted by passing them through 25 g needle. Phagosomes and endosomes were

purified by magnetic separation, washed, and lysed. 5 μg of proteins were submitted to separation on a 10% SDS NuPAGE Bis-Tris gels (Invitrogen). Proteins were transferred on a PVDF membrane and immunodetection was realized. Rabbit pAb anti-TLR9 (Santa Cruz), mouse anti-human transferrin receptor, rat anti-LAMP2, and mouse mAb anti-AEP were from PharMingen and R&D Systems, respectively.

Protease activity assays were performed on a FluoStar Optima (BMG labtech) by measuring the release of fluorescent N-Acetyl-Methyl-Coumarin in citrate buffer (pH 5.5) at 37°C. Specific substrates for AEP (Z-Ala-Ala-Asn-NHMec), CatB (Z-Arg-Arg-NHMec), CatB/L (Z-Phe-Arg-NHMec), and CatS (Z-Val-Val-Arg-NHMec) were from Bachem.

For immunoprecipitation of CatB, L, and S, 100 μg of protein were labeled with 10 μM of DCG-04 (kind gift by H. Overkleeft, Leiden, Netherlands) for 60 min at 37°C. Reaction was stopped by adding sample buffer and boiling in 1% SDS. Samples were analyzed by 12% SDS-NuPAGE and developed with HRP-coupled streptavidin (Amersham).

Complementation assays were performed by adding 0.2 μg/10^6 cells of pro-CatK to AEP-deficient DCs 30 min before stimulation with different concentrations of CpG. Rabbit pAb anti-CatK was from Santa Cruz.

Endosomal pH Measurement

Endosomal pH measurement has been described (Savina et al., 2006). In brief, cells were pulsed with 1 mg/ml of FITC- and Alexa-647-labeled 40 kDa dextrans (Molecular Probes) for 10 min at 37°C and extensively washed with cold PBS plus 1% BSA. Cells were then chased for different times and analyzed by FACS, via a FL1/FL4 gate selective for cells that have endocytosed the fluorescent probes.

Phagosomal OVA Degradation Assay

3 μm NH2-latex beads (Polyscience, Inc) were covalently coated with OVA (0.5 mg/ml) according to manufacturer's instructions. BMDCs were pulsed for 10 min at 37°C and chased for different times at 37°C. Cells were lysed in 50 mM Tris-HCl (pH 7.4) supplemented with 150 mM NaCl, 1 mM DTT, 0.5% NP-40, and cocktail of protease inhibitors (Roche). For FACS analysis, latex beads were stained with polyclonal anti-OVA (Sigma) and a secondary anti-rabbit Alexa 647 (Molecular Probes).

^{35}S Labeling of TLR9 Protein, Site-Directed Mutagenesis, Digestion Assays, and Transfection in DCs

Mouse *Tlr9* cDNA (Invivogen) construct was fused at the C terminus to GFP (pEGFP-N1) and generated by sequential PCR with the primers 5′-ccgctagccc-caccATGGTTCTCCGTCGAAGGA-3′ (forward) and 5′-cgtcgactgcagaattcgaag ctTTTCTGCTGTAGGTCCCCGGCAG-3′ (reverse). The recombinant C-terminal *Tlr9* fragment encompassing the residues 471–1032 was generated as previously described (Park et al., 2008). All constructs were cloned into pcDNA3.1 (+) (Invitrogen). *Tlr9* cDNA was mutated with the quick change Mutagenesis Kit (Stratagene) according to the manufacturer's conditions. For mutagenesis of Asn 466, sense primer 5′-GCTTCTAAGCAGTTCATGGACAGG-3′ and antisense primer 5′-CCTGTCCATGAACTGCTTAGAAGC-3′ were used. *Tlr9* GFP was transcribed and translated in vitro with TNT T7 quick Coupled Transcription/Translation system (Promega) and 10 μCi (^{35}S)methionine (Perkin Elmer). Digestion assays were performed at 37°C in 50 mM citrate buffer (pH 5.5), 0.1% CHAPS, 1 mM DTT, together with 5 μl of translation reaction and recombinant proteases (AEP, kindly given by C. Watts, Dundee, UK; CatB, D, K, L, and S from Calbiochem), or 20 μg of total lysate from WT or AEP-deficient BMDCs in the absence or presence of the inhibitors: leupeptin 1 mM or MV026630 (50 μM).

10^6 BMDCs at day 8 were transfected with 1 μg of cDNA coding for GFP, GFP-tagged *Tlr9*, N466Q, or C-terminal *Tlr9* fragment via the Amaxa kit (Lonza, Germany). 24 hr later, cells were harvested and stimulated with TLR agonists.

Statistical Analysis

Statistical significance was determined by unpaired t test or one-way ANOVA. *$p < 0.05$, **$p < 0.01$, and ***$p < 0.001$.

SUPPLEMENTAL DATA

Supplemental Data include six figures and can be found with this article online at http://www.cell.com/immunity/supplemental/S1074-7613(09)00450-6.

ACKNOWLEDGMENTS

We are grateful to S. Akira (Osaka, Japan) for providing *Tlr9*$^{-/-}$ and *Myd88*$^{-/-}$ mice (MTA) and H. Ploegh and B. Park (MIT, USA) for providing the cDNA encoding for the C-terminal *Tlr9* fragment. We are especially grateful to C. Peters (Freiburg, Germany) and I. Werber for providing AEP-deficient mice. This study was funded by grants from l'Institut National de Santé et Recherche Médicale (AVENIR fellowship) and La Mairie de Paris to B.M. and fellowships to F.E.S. (Marie Curie Training network MRTN-CT-2004-512585 and ARC), to S.M. (ANR), and to R.C. (Région d' Ile de France).

Received: February 25, 2009
Revised: June 26, 2009
Accepted: September 11, 2009
Published online: October 29, 2009

REFERENCES

Ahmad-Nejad, P., Hacker, H., Rutz, M., Bauer, S., Vabulas, R.M., and Wagner, H. (2002). Bacterial CpG-DNA and lipopolysaccharides activate Toll-like receptors at distinct cellular compartments. Eur. J. Immunol. *32*, 1958–1968.

Asagiri, M., Hirai, T., Kunigami, T., Kamano, S., Gober, H.J., Okamoto, K., Nishikawa, K., Latz, E., Golenbock, D.T., Aoki, K., et al. (2008). Cathepsin K-dependent toll-like receptor 9 signaling revealed in experimental arthritis. Science *319*, 624–627.

Barnden, M.J., Allison, J., Heath, W.R., and Carbone, F.R. (1998). Defective TCR expression in transgenic mice constructed using cDNA-based alpha- and beta-chain genes under the control of heterologous regulatory elements. Immunol. Cell Biol. *76*, 34–40.

Bell, J.K., Mullen, G.E., Leifer, C.A., Mazzoni, A., Davies, D.R., and Segal, D.M. (2003). Leucine-rich repeats and pathogen recognition in Toll-like receptors. Trends Immunol. *24*, 528–533.

Brinkmann, M.M., Spooner, E., Hoebe, K., Beutler, B., Ploegh, H.L., and Kim, Y.M. (2007). The interaction between the ER membrane protein UNC93B and TLR3, 7, and 9 is crucial for TLR signaling. J. Cell Biol. *177*, 265–275.

Chen, J.M., Dando, P.M., Rawlings, N.D., Brown, M.A., Young, N.E., Stevens, R.A., Hewitt, E., Watts, C., and Barrett, A.J. (1997). Cloning, isolation, and characterization of mammalian legumain, an asparaginyl endopeptidase. J. Biol. Chem. *272*, 8090–8098.

Chen, J.M., Dando, P.M., Stevens, R.A., Fortunato, M., and Barrett, A.J. (1998). Cloning and expression of mouse legumain, a lysosomal endopeptidase. Biochem. J. *335*, 111–117.

Delamarre, L., Pack, M., Chang, H., Mellman, I., and Trombetta, E.S. (2005). Differential lysosomal proteolysis in antigen-presenting cells determines antigen fate. Science *307*, 1630–1634.

Duramad, O., Fearon, K.L., Chang, B., Chan, J.H., Gregorio, J., Coffman, R.L., and Barrat, F.J. (2005). Inhibitors of TLR-9 act on multiple cell subsets in mouse and man in vitro and prevent death in vivo from systemic inflammation. J. Immunol. *174*, 5193–5200.

Ewald, S.E., Lee, B.L., Lau, L., Wickliffe, K.E., Shi, G.P., Chapman, H.A., and Barton, G.M. (2008). The ectodomain of Toll-like receptor 9 is cleaved to generate a functional receptor. Nature *456*, 658–662.

Fiebiger, E., Maehr, R., Villadangos, J., Weber, E., Erickson, A., Bikoff, E., Ploegh, H.L., and Lennon-Dumenil, A.M. (2002). Invariant chain controls the activity of extracellular cathepsin L. J. Exp. Med. *196*, 1263–1269.

Guiducci, C., Ghirelli, C., Marloie-Provost, M.A., Matray, T., Coffman, R.L., Liu, Y.J., Barrat, F.J., and Soumelis, V. (2008). PI3K is critical for the nuclear translocation of IRF-7 and type I IFN production by human plasmacytoid predendritic cells in response to TLR activation. J. Exp. Med. *205*, 315–322.

Hemmi, H., and Akira, S. (2005). TLR signalling and the function of dendritic cells. Chem. Immunol. Allergy *86*, 120–135.

Hou, B., Reizis, B., and DeFranco, A.L. (2008). Toll-like receptors activate innate and adaptive immunity by using dendritic cell-intrinsic and -extrinsic mechanisms. Immunity *29*, 272–282.

Jancic, C., Savina, A., Wasmeier, C., Tolmachova, T., El-Benna, J., Dang, P.M., Pascolo, S., Gougerot-Pocidalo, M.A., Raposo, G., Seabra, M.C., and Amigorena, S. (2007). Rab27a regulates phagosomal pH and NADPH oxidase recruitment to dendritic cell phagosomes. Nat. Cell Biol. *9*, 367–378.

Kaisho, T., and Akira, S. (2001). Dendritic-cell function in Toll-like receptor- and MyD88-knockout mice. Trends Immunol. *22*, 78–83.

Kawai, T., and Akira, S. (2006). TLR signaling. Cell Death Differ. *13*, 816–825.

Kim, Y.M., Brinkmann, M.M., Paquet, M.E., and Ploegh, H.L. (2008). UNC93B1 delivers nucleotide-sensing toll-like receptors to endolysosomes. Nature *452*, 234–238.

Latz, E., Verma, A., Visintin, A., Gong, M., Sirois, C.M., Klein, D.C., Monks, B.G., McKnight, C.J., Lamphier, M.S., Duprex, W.P., et al. (2007). Ligand-induced conformational changes allosterically activate Toll-like receptor 9. Nat. Immunol. *8*, 772–779.

Lennon-Dumenil, A.M., Roberts, R.A., Valentijn, K., Driessen, C., Overkleeft, H.S., Erickson, A., Peters, P.J., Bikoff, E., Ploegh, H.L., and Wolf Bryant, P. (2001). The p41 isoform of invariant chain is a chaperone for cathepsin L. EMBO J. *20*, 4055–4064.

Lennon-Dumenil, A.M., Bakker, A.H., Maehr, R., Fiebiger, E., Overkleeft, H.S., Rosemblatt, M., Ploegh, H.L., and Lagaudriere-Gesbert, C. (2002). Analysis of protease activity in live antigen-presenting cells shows regulation of the phagosomal proteolytic contents during dendritic cell activation. J. Exp. Med. *196*, 529–540.

Li, D.N., Matthews, S.P., Antoniou, A.N., Mazzeo, D., and Watts, C. (2003). Multistep autoactivation of asparaginyl endopeptidase in vitro and in vivo. J. Biol. Chem. *278*, 38980–38990.

Loak, K., Li, D.N., Manoury, B., Billson, J., Morton, F., Hewitt, E., and Watts, C. (2003). Novel cell-permeable acyloxymethylketone inhibitors of asparaginyl endopeptidase. Biol. Chem. *384*, 1239–1246.

Maehr, R., Hang, H.C., Mintern, J.D., Kim, Y.M., Cuvillier, A., Nishimura, M., Yamada, K., Shirahama-Noda, K., Hara-Nishimura, I., and Ploegh, H.L. (2005). Asparagine endopeptidase is not essential for class II MHC antigen presentation but is required for processing of cathepsin L in mice. J. Immunol. *174*, 7066–7074.

Manoury, B., Hewitt, E.W., Morrice, N., Dando, P.M., Barrett, A.J., and Watts, C. (1998). An asparaginyl endopeptidase processes a microbial antigen for class II MHC presentation. Nature *396*, 695–699.

Manoury, B., Mazzeo, D., Fugger, L., Viner, N., Ponsford, M., Streeter, H., Mazza, G., Wraith, D.C., and Watts, C. (2002). Destructive processing by asparagine endopeptidase limits presentation of a dominant T cell epitope in MBP. Nat. Immunol. *3*, 169–174.

Manoury, B., Mazzeo, D., Li, D.N., Billson, J., Loak, K., Benaroch, P., and Watts, C. (2003). Asparagine endopeptidase can initiate the removal of the MHC class II invariant chain chaperone. Immunity *18*, 489–498.

Matsumoto, F., Saitoh, S., Fukui, R., Kobayashi, T., Tanimura, N., Konno, K., Kusumoto, Y., Akashi-Takamura, S., and Miyake, K. (2008). Cathepsins are required for Toll-like receptor 9 responses. Biochem. Biophys. Res. Commun. *367*, 693–699.

Park, B., Brinkmann, M.M., Spooner, E., Lee, C.C., Kim, Y.M., and Ploegh, H.L. (2008). Proteolytic cleavage in an endolysosomal compartment is required for activation of Toll-like receptor 9. Nat. Immunol. *9*, 1407–1414.

Rutz, M., Metzger, J., Gellert, T., Luppa, P., Lipford, G.B., Wagner, H., and Bauer, S. (2004). Toll-like receptor 9 binds single-stranded CpG-DNA in a sequence- and pH-dependent manner. Eur. J. Immunol. *34*, 2541–2550.

Savina, A., Jancic, C., Hugues, S., Guermonprez, P., Vargas, P., Moura, I.C., Lennon-Dumenil, A.M., Seabra, M.C., Raposo, G., and Amigorena, S. (2006). NOX2 controls phagosomal pH to regulate antigen processing during crosspresentation by dendritic cells. Cell *126*, 205–218.

Shirahama-Noda, K., Yamamoto, A., Sugihara, K., Hashimoto, N., Asano, M., Nishimura, M., and Hara-Nishimura, I. (2003). Biosynthetic processing of cathepsins and lysosomal degradation are abolished in asparaginyl endopeptidase-deficient mice. J. Biol. Chem. *278*, 33194–33199.

Trombetta, E.S., Ebersold, M., Garrett, W., Pypaert, M., and Mellman, I. (2003). Activation of lysosomal function during dendritic cell maturation. Science *299*, 1400–1403.

Uhlmann, F., Wernic, D., Poupart, M.A., Koonin, E.V., and Nasmyth, K. (2000). Cleavage of cohesin by the CD clan protease separin triggers anaphase in yeast. Cell *103*, 375–386.

Yi, A.K., Tuetken, R., Redford, T., Waldschmidt, M., Kirsch, J., and Krieg, A.M. (1998). CpG motifs in bacterial DNA activate leukocytes through the pH-dependent generation of reactive oxygen species. J. Immunol. *160*, 4755–4761.